Electrical alternative to pulsed fiber-delivered lasers in microsurgery

Daniel Palanker,[a] Igor Turovets, and Aaron Lewis
Laser Center, Hadassah University Hospital, P.O. Box 12000, Jerusalem 91120, and NanoMed Ltd., Jerusalem, Israel

(Received 15 October 1996; accepted for publication 7 March 1997)

An electrical system based on a tapered microelectrode has been developed for generation of high voltage sub-microsecond discharge in physiological medium. Different types of the resulting pulses of current are investigated as well as the dynamics of the associated cavitation bubbles. A highly localized zone of power dissipation—about 20 μm in size—results in a low threshold energy of cavitation bubble generation—about 3 μJ—in comparison to laser-based intraocular microsurgical instrumentation with fiber delivery systems. Cavitation bubble dynamics resulting from the electric discharge is similar to that observed with ns-pulsed fiber-delivered lasers in strongly absorbing liquid medium. Efficiency of the pulse energy conversion to the bubble energy is about 12%, which is lower than the best results obtained with lasers. In spite of that, due to the low threshold energy, cavitation bubbles required for effective cutting of soft tissue can be generated at energies lower than that used in laser instrumentation with fiber-based delivery systems. The proposed device has a potential to become a convenient and a cost-effective alternative to such lasers in vitreoretinal microsurgery. © *1997 American Institute of Physics.* [S0021-8979(97)08111-5]

I. INTRODUCTION

Various pulsed lasers have been applied to soft tissue cutting and removal in liquid environment. The mechanism of tissue cutting with such lasers is generally associated with absorption of a short laser pulse accompanied by an explosive expansion of the overheated liquid and cavitation bubble formation. As a result of such process, the tissue in the light absorption zone, as well as in the area of fast expansion and collapse of the cavitation bubble is disrupted.[1–3] There are three different mechanisms of light absorption that have been involved in pulsed laser surgery. These are:

(i) linear absorption of light by the tissue,[1,4]
(ii) linear absorption of light by the medium,[2,5,6] and
(iii) nonlinear absorption by tissue or medium associated with dielectric breakdown of the material.[3,7]

In spite of differences in the mechanism of laser radiation absorption, the tissue cutting in all these approaches was associated with the cavitation bubble formation.

In view of the general complicated nature of laser-based devices we have searched for ways to emulate this mechanism of cavitation bubble generation by nonlaser methodologies. Since such cavitation bubbles result from local and fast heat energy deposition it is logical to consider an overheating of a conductive medium with a short pulse of electric current. In this article we demonstrate that such an electromicrosurgical cavitation can be realized in physiological media with the potential for applications in ophthalmology. Previous investigators who have considered pulsed electrical techniques and have seen cavitation bubble formation[8,9] considered these bubbles either as an undesirable side effect[9] or as a means for shock wave generation for hard tissue destruction.[8] These electrosurgical devices were designed for relatively high energy pulse generation: between 25 mJ and 40 J and with relatively long pulse duration: hundreds of microseconds. Such high energy pulses resulting in a few millimeter-sized cavitation bubbles cannot be applied to eye microsurgery. Laser-based techniques indicate that the pulse energies required for such applications are in the range of a few tens of micro Joules and the pulse duration generally are in a sub-microsecond range.[10,11] In addition to these time/energy characteristics it is required that any device for vitreoretinal surgery should be able to withstand tens of thousands of pulses. The previous high energy devices have a lifetime of less than 100 pulses.[8]

The device described in this article is based on a microelectrode and corresponding pulse generator that could become an alternative to fiber-delivered lasers in vitreoretinal surgery. We investigate in this work the different mechanisms of discharge generated by this device in physiological medium and the dynamics of the associated cavitation bubbles.

II. THEORETICAL CONSIDERATIONS

A primary goal was to develop electrode geometry similar to that of the laser tips that have been applied to the laser-assisted microsurgery of the eye.[2,10] This was achievable with techniques that have been developed to produce a thin platinum wire sealed into a tapered glass pipette[12] with the diameter varying between 0.7 mm in its cylindrical part and 0.2 mm at the tip [see Fig. 1(a)]. The exit surface of this electrode was a flat inlaid metal disk of a few tens of micrometers in diameter. This electrode was connected to the output of a HV pulse generator schematically shown in Fig. 1(b). The second electrode, connected to a common output, was accomplished as a concentric stainless steel needle with an outer diameter of 1 mm.

To achieve high cutting efficiency, cavitation bubbles should be created fast enough for generation of high pressures and high boundary velocity and acceleration. This re-

[a]Address for correspondence: W.W. Hansen Experimental Physics Laboratory, Free Electron Laser Center, Stanford University, Stanford, CA 94305-4085; Electronic mail: palanker@leland.stanford.edu

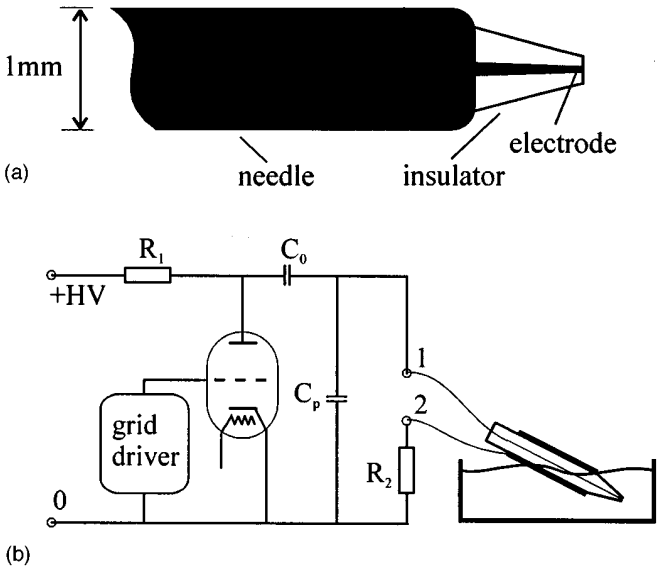

FIG. 1. (a) Schematic representation of the electrode geometry. (b) Schematic representation of the HV pulse generator. The small internal electrode was connected to the negative output of the generator (point 1), whereas the external needle was connected to the common output (point 2).

quirement determines the minimal peak power of the pulse. On the other hand, the cutting action should be local enough for prevention of extensive damage in the surrounding of the application site. This requirement limits the total energy that can be used for the bubble formation. Based on the experience of laser-induced cavitation,[1,10] the diameter of the cavitation bubble required for precise and effective cutting of vitreoretinal tissue should be in a range of 0.4–0.5 mm and this corresponds to bubble energies in the range of 3–6 μJ. The threshold energy of cavitation bubble formation can be estimated as the energy required for the heating of the infinitesimal thin water layer adjacent to the electrode to 100°C.[13] This energy is determined by the radius of the electrode [see Eq. (A3) in the Appendix]. For obtaining a threshold energy of about 5 μJ (which is less than the threshold characteristic for laser-based instrumentation[2,14]) the electrode radius a should be about 13 μm (see Appendix). Resistance R_e of the physiological medium also depends on the radius of the electrode [Eq. (A1) in the Appendix] and for $a=13$ μm it will be about 7 kΩ in Hartmann's solution (see the Appendix). The parasitic heat transfer from water to the metal wire is determined by the electrode dimensions and duration of heating Eq. (A4) in the Appendix]. Thus, to limit such heat transfer during the pulse by 5% of the discharge energy, the pulse duration should be limited by about 0.3 μs (see the Appendix). The pulse duration is determined by the discharging capacitance C and the resistance of the circuit: $\tau=R_eC$. Thus, for obtaining the discharge duration $\tau=0.3$ μs, C should be about 40 pF. For obtaining a discharge energy $E=5\mu$J, the charging potential U of the capacitance C should be about 500 V [see Eq. (A5) in the Appendix].

III. MATERIALS AND METHODS

For realization of the proposed idea we used a homemade HV pulse generator based on a thyratron switch that enables a fast discharge of the capacitor C_0 (14pF) on an external load [see Fig. 1(b)]. When a thyratron was switched on, a short (30 ns rise time) a negative pulse was generated at the electrode resulting from the discharge of the capacitance through the electrolyte. The pulse generator and the cables inevitably have some parasitic capacitance C_p (about 30 pF in our case), so the resulting voltage on the electrode, U_-, was lower than the starting voltage U_0 on the discharge capacity C_0:

$$U_- = U_0 C_0/(C_0+C_p) \approx 0.3 U_0 .$$

Duration of this negative pulse was $\tau_- = R_e(C_0+C_p) \approx 0.3$ μs. After switching the thyratron off, the capacitor C_0 was slowly charged back to the potential U_0 through the resistor R_1 (10 MΩ) and through the solution. At this stage the pulse polarity was positive and the pulse duration was $\tau_+ = (R_1+R_e)C_0 \approx$ 140 μs. The amplitude of the electrode potential during this pulse can be estimated as follows:

$$U_+ = U_0 R_e/(R_1+R_e) \approx 0.001 U_0 .$$

The electrode potential (U) was measured [in point 1, Fig. 1(b)] with the P6015 Tektronix HV probe (1000×, 3pF, 100 MΩ). The current was measured as a voltage drop on a resistor $R_2=100$ Ω connected between the external electrode and the common output of the generator [point 2, Fig. 1(b)] with the P6139A Tektronix probe (10×, 8 pF, 10 MΩ). The voltage and current pulses were registered simultaneously by the Tektronix TDS 520 digital oscilloscope (500 MHz), and the data was transferred to the computer for analysis. In order to reduce the noise of the measured current we applied a 20 MHz filtering that resulted in some delay (about 30 ns) of the current relative to the signal of the electrode potential.

The diameter of the wire at the exit of the electrode was 25 μm. As the electrode was produced as an insulated wire placed inside a concentric metal needle, it had some capacitance (about 5 pF in our case). The current charging this capacitance (I_c) caused an energy dissipation distributed along the side walls of the electrode, whereas the current passing through the exit surface of the electrode (I) resulted in heating of the solution in front of the exit surface. Thus, in order to make the correct measurements of this current we subtracted the I_c (separately measured in the air) from the total current passing through the electrode in the solution: $I = I_{tot} - I_c$. The capacitance-originated current inside the solution was slightly (up to 10%) greater than in the air due to the fact that the tapered part of the electrode exiting from the needle [see Fig. 1(a)] had some additional capacitance inside the solution.

We used a standard Hartmann's solution as a physiological medium. Photographs of the discharge were taken on an inverted microscope with ×50 objective using a charge coupled device (CCD) camera (LN/CCD-512-TKB/1, Princeton Instruments, Inc.). The fast flash photography of cavitation bubbles has been accomplished with a ×10 objective using a SLL-250 flash lamp-pumped dye laser (Candela Corp., Wayland, USA). The pulse duration of this laser was about 0.5 μs, the delay between the electric pulse and the light pulse has been varied using a delay generator DDT-20 (Candela Corp.).

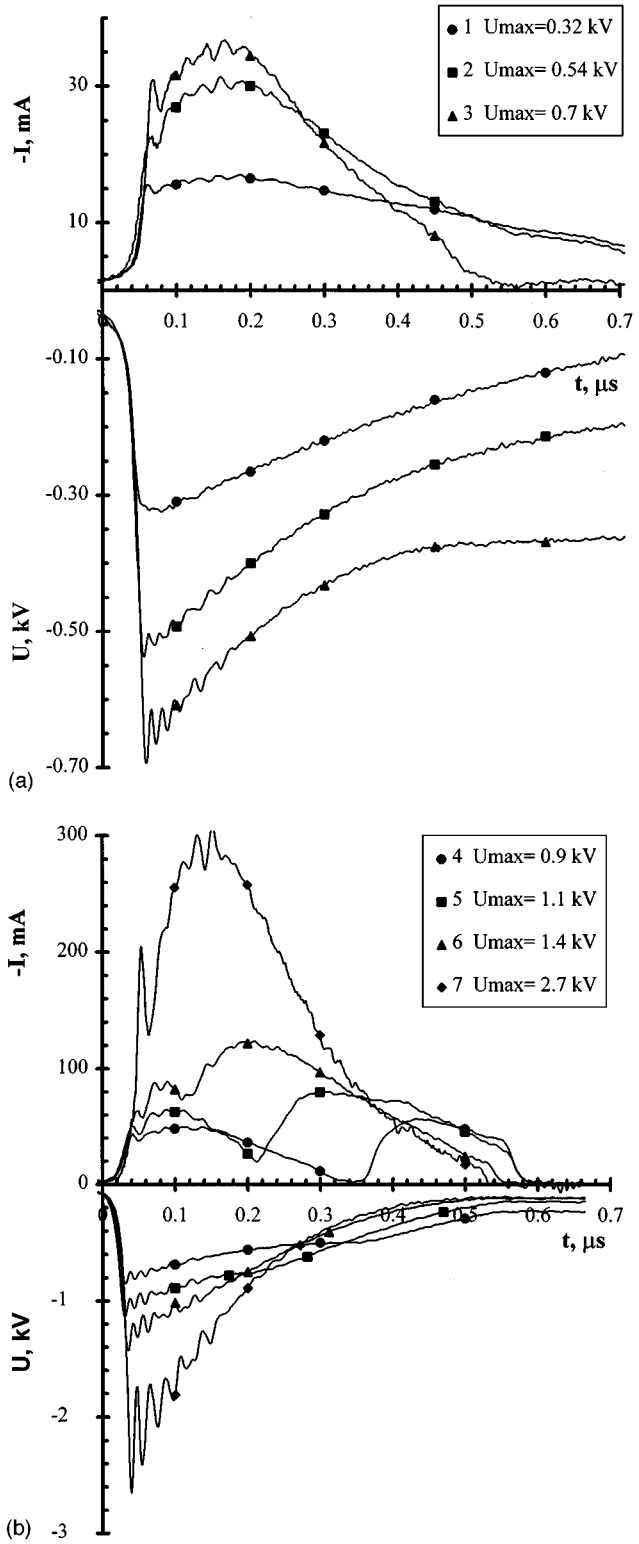

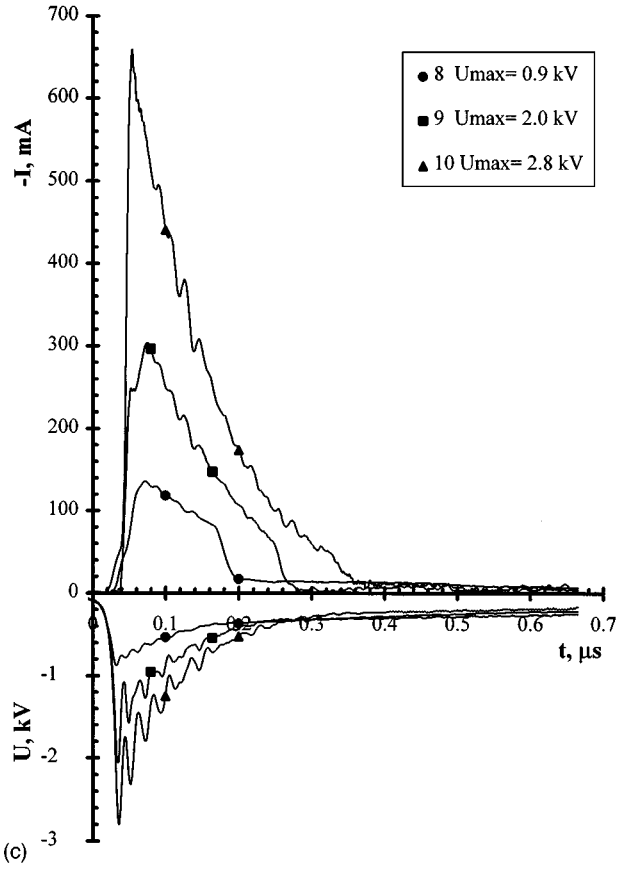

FIG. 2. Time dependence of the electrode potential (U) and current passing through the exit surface of the electrode ($-I$) during the discharge. The current is presented at positive polarity for convenience of observation. The delay (about 30 ns) in the start of the current relative to the voltage results from filtering of the current signal. (a) Discharge starts in liquid. Note the complete switching off of the discharge at $U_{max}=0.7$ kV, when the current becomes zero at non-zero potential (curve 3, t $\approx$ 0.55 μs). (b) Discharge starts in liquid. Note the second pulse of current and corresponding drop of the voltage after the switching off of the current at 0.32 μs on curve 4. With the increase of the electrode potential a second pulse was generated earlier and two pulses of current overlap, becoming indistinguishable. (The short peak of current at 60 ns is a remnant of the electrode capacitance-originated current). (c) Discharge starts inside the small oxygen bubble sitting on the electrode. The peaks of current are about twice as shorter and higher than corresponding peaks of the discharge starting in liquid (b).

IV. RESULTS

The resulting pulse profiles of the electrode potential (U) and the current passing through the exit surface of the electrode (I) are presented on Fig. 2. At $U_{max}=0.3$ kV [Fig. 2(a), curves 1] the voltage and current simultaneously decrease with a time constant of about 0.6 μs. As the potential increases, the nature of the discharge changes: The current drops much faster after about 0.2 μs, resulting in slowing down the voltage reduction [Fig. 2(a), curves 2]. At $U_{max}=0.7$ kV [Fig. 2(a), curves 3], the current falls to zero (switched off) when the potential is still at the half of the maximum. This switching off of the current results from gas generation on the surface of electrode that disconnects the liquid from the metal surface.

At higher electrode potentials the second pulse of current is generated after the first one [see Fig. 2(b)], and with an

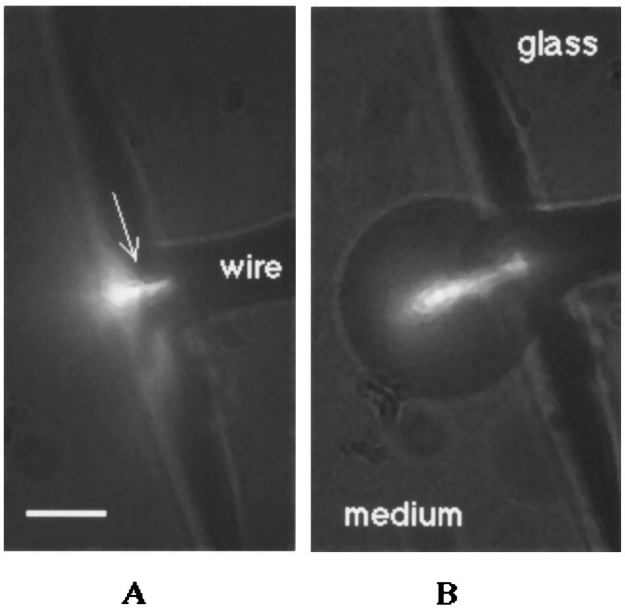

FIG. 3. Micrographs of the sparks generated during the discharge. Original magnification is ×500. The wire diameter at the exit is 20 μm. Bar = 20 μm. (a) Typical discharge at U_{max} = 2.7 kV in liquid. Lighted area with dimensions of about 7 μm emits reddish light in front of the electrode. Reflection of this light on the electrode exit surface is seen at the right of the arrow. (b) Typical spark generated inside the oxygen bubble remained on the tip after the previous pulse application. The spark length seems to be shorter than the bubble diameter as it reaches the boundary above or below the bubble's equator.

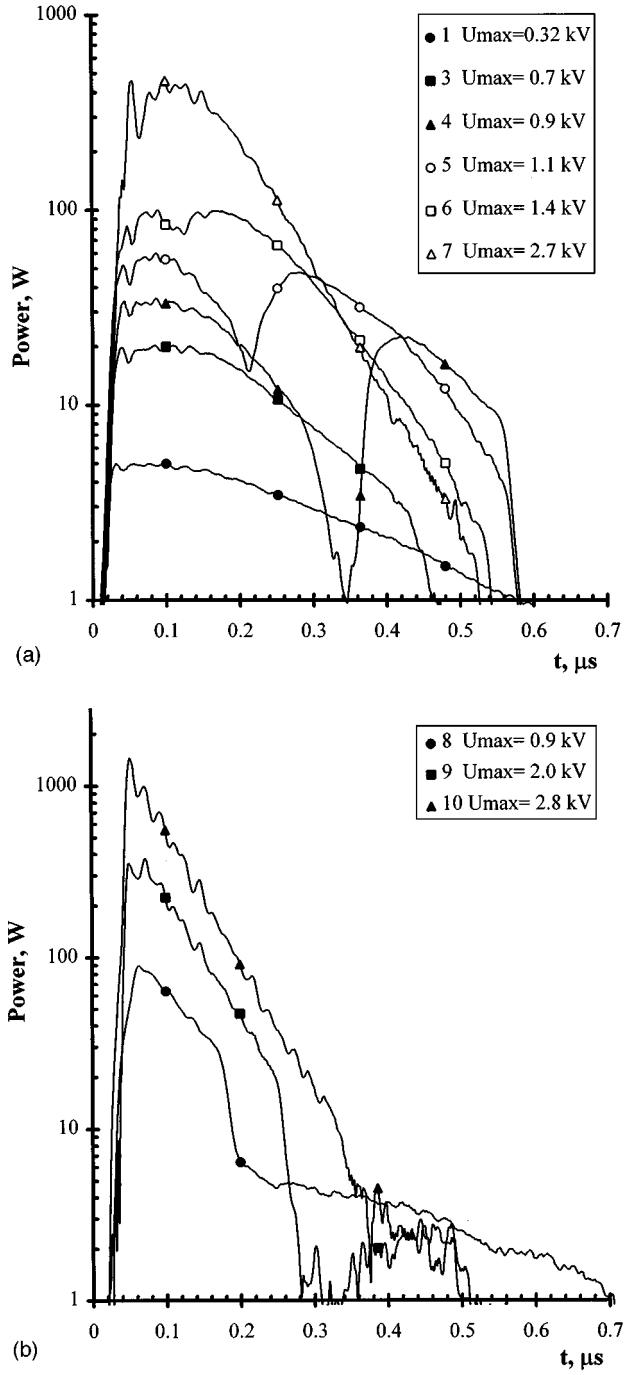

FIG. 4. Power dissipation in the liquid in front of the electrode at different starting potentials. These curves are the result of multiplication of the corresponding values of the voltage on current at each moment of time presented in Fig. 2. (a) Discharge starts in liquid. The curves have a flat top with duration of about 100 ns, and the exponential decay area reaching a value of 60 ns at U_{max} = 2.7 kV (curve 7). (b) Discharge starts inside the oxygen bubble. The curves have no flat top, and the exponential decay has the time constant of about 60 ns at all starting potentials.

increase of voltage the delay between these two pulses decreases. At U_{max} higher than 1.4 kV [Fig. 2(b), curves 6], these two pulses completely overlap and at U_{max}=2.7 kV [Fig. 2(b), curves 7], they became indistinguishable. (The sharp peak at 60 ns is the remnant of the capacitance-originated current through the walls of the electrode.) The discharge at a voltage range of 1.4–2.7 kV was accompanied by emission of the reddish light [see Fig. 3(a)] and sound wave generation. At U_{max}=2.7 kV, the radius of the light spot was about 7 μm.

As was mentioned above, each fast discharge of the capacitor (when the central electrode played the role of the cathode) was accompanied by a slow charging phase during which it became an anode. The electrode potential at this phase did not exceed a few volts and the pulse duration was about 140 μs. At this stage oxygen generated on the electrode was accumulated in the bubble (50 μm in diameter at U_{max}=2.7 kV) that was slowly dissolving and rising up in the solution. When the electric pulses were generated at a repetition rate exceeding 10 Hz these bubbles did not have enough time to move away between the pulses. In this case a discharge could start in the gaseous phase, as can be seen in Fig. 3(b). This discharge was shorter and had a higher peak power [see Fig. 2(c)] than in the case of a discharge starting in a liquid environment [Fig. 2(b)]. However, the total energy released during the discharge at the same voltage in these two cases remained the same. An interesting feature of the discharge starting in gas was that after the voltage dropped below the threshold and the gas discharge was switched off, there is still some nonzero current. Such behavior probably indicates that the gas-containing insoluble bubble covered only a part of the electrode enabling some discharge into the liquid also.

The curves of power dissipation ($W = U \times I$) in a liquid and in a gas bubble are presented in Figs. 4(a) and 4(b), respectively in a semi-logarithmic scale. The discharge starting in liquid had a duration full width half maximum

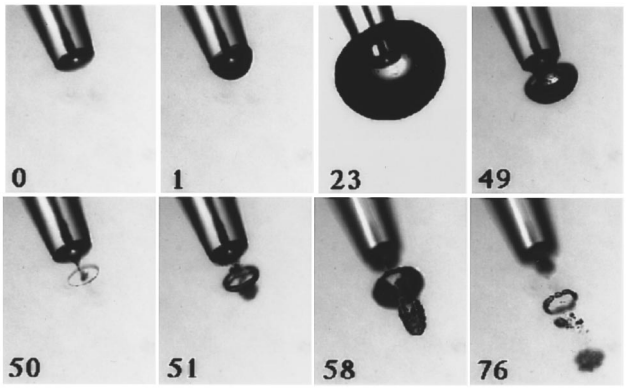

FIG. 5. Sequence of micrographs presenting the dynamics of cavitation bubbles generated at U_{max} = 2.7 kV. The tip diameter is 200 μm and original magnification is 100×. The delay between the electric pulse and the flash pulse is shown in the corner of each frame (in μs). The tip was held at an angle (about 15°) with the horizon, as it is schematically shown in Fig. 1(b), thus only a central part of the picture is seen in focus.

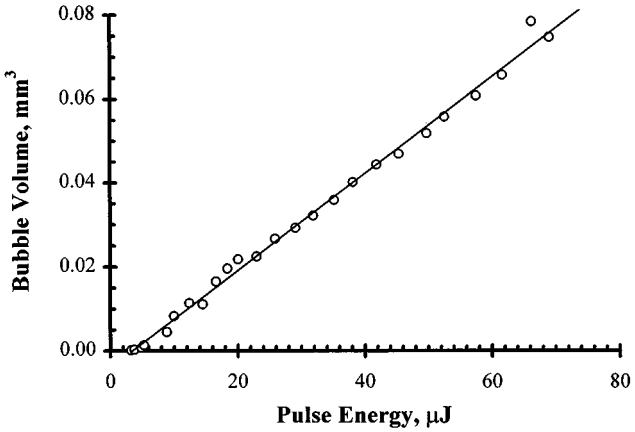

FIG. 6. Dependence of the maximal volume of the primary cavitation bubble on the pulse energy. The wire diameter was 20 μm. The intersection of the linear approximation of the curve with abscissa — 3.3 μJ — represents the threshold energy of the cavitation bubble generation.

(FWHM) that varied between 300 ns at the U_{max}=0.3 kV (curve 1) and about 150 ns at U_{max}=2.7 kV (curve 7). At this voltage, the pulse profile had a flat top of about 100 ns duration followed by the exponential decay area with a time constant of about 60 ns. The power profile of the discharge starting in a gas bubble had no flat top, and the time constant of the exponential decay area was about 60 ns at U_{max} varying between 0.9 and 2.9 kV [curves 8–10, Fig. 4(b)].

During an application of a large amount of pulses degradation of the electrodes was observed, i.e., the wire was etched inside the insulator. The rate of etching depended not only on amount of charge transferred, but also on the voltage applied. Deepening of the pit in front of the wire resulted in an increase of the probability that it will be filled with gas, and at some stage only a discharge starting in gas was observed. When this pit became so deep that the electric field across it was lower than the threshold required for gas discharge ignition, the discharge was terminated. This phenomenon determines the lifetime of the electrode. For example, at U_{max}=2.4 kV the electrode withstands about 300 000 pulses. During this period the wire had been etched to about 40 μm in depth and the resulting cavity prevented the discharge. The average metal expenditure rate was about 5×10^{-12} g per pulse, or about 25 electron charge units per atom of Pt.

A. Cavitation bubble dynamics

The sequence of micrographs of cavitation bubbles generated at the electrode with a 20 μm wire at U_{max}=2.7 kV is shown in Fig. 5. The delay time between the electric pulse and the flash of dye laser is shown (in μs) in the corner of each frame. The spark generated in the vicinity of the electrode is clearly seen as a white spot in front of the wire. The average velocity of the bubble boundary during the first 1 μs of the growth phase (frames 1,2) was about 90 m/s. The primary cavitation bubble grew in about 25 μs (frames 2,3), reaching the maximal diameter of about 0.5 mm. During the collapse the bubble had a mushroom-like shape (frame 4), that was eventually transformed to a ring and a stem connecting its center with the center of the tip (frame 5). The secondary bubbles were generated from both, the ring and the stem (frames 6,7). These bubbles were ejected away from the tip at different velocities (about 5 and 17 m/s, respectively) and then collapsed and disappeared at the distances of about 0.25 and 0.65 mm, respectively, at about 76 μs after the pulse (frame 8). The maximal volume of the primary cavitation bubble linearly increased with the pulse energy (see Fig. 6). The threshold energy of bubble generation, E_{thresh}, which is a point of intersection of the linear approximation of the graph with the abscissa, is about 3.3 μJ. Efficiency of the discharge energy conversion to the energy of the cavitation bubble $[E_{bub}/(E_{pulse} - E_{thresh})]$ is about 12%. (The energy of the bubble is estimated as $E_{bub}=P\cdot V_{max}$,[15] where P is the atmospheric pressure, and V_{max} is the maximal volume of the bubble).

V. DISCUSSION

The nature of the observed discharges becomes more clear analyzing the resistance of the system ($R=U/I$, Fig. 7). The graphs shown in Fig. 7 were obtained by division of the electrode potential (U) on the current (I), presented in Fig. 2, thus the same indices of the curves correspond to the same experimental conditions. The resistance is infinite at the beginning of the pulse and reduces during the first ~30 ns due to the delay in the current signal relative to the potential resulting from filtering, as it was mentioned above. Thus, the graphs of resistance are depicted starting from 40 ns. At low potential [U_{max}=0.3 kV, Fig. 7(a), curve 1] the resistance reduces from 22 to 13 kΩ during the pulse, which probably results from heating of the solution. Reduction of the resistance at the beginning of the pulse becomes faster at higher voltage (curves 2, 4), as the medium is heated faster at higher discharge power. The resistance during the first pulse of current is more than twice as high than the theoretical estimations described above. The discrepancy is probably associated with the formation of a high resistivity sheath with low ion concentration near the electrode at high voltage pulse application.[16] As the potential increases, the gas generation

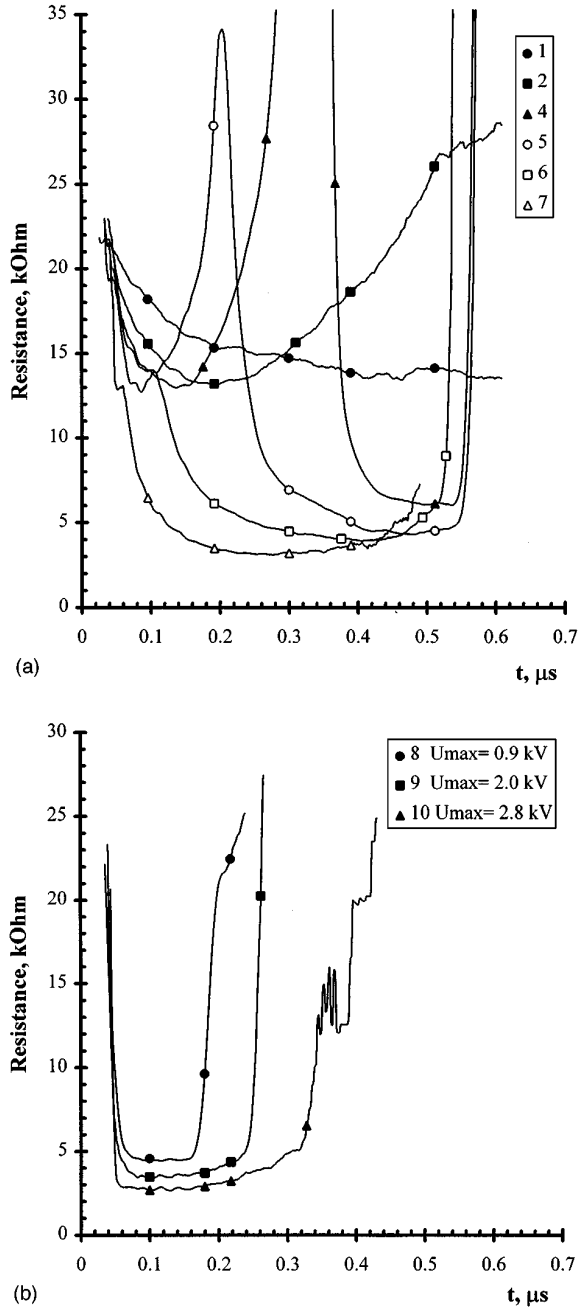

FIG. 7. Time dependence of the resistance of the discharge. These curves are the result of division of the voltage on the current presented in Fig. 2. The signal starts at infinity due to the delay of the current relative to the voltage resulting from filtering of the current signal. (a) Discharge starts in liquid. 1: U_{max}=0.32 kV, 2: U_{max}=0.54 kV, 4: U_{max}=0.9 kV, 5: U_{max}=1.1 kV, 6: U_{max}= 1.4 kV, 7: U_{max}=2.7 kV. Switching off of the discharge is clearly seen by a sharp increase of the resistance (curves 2,4,5). Transition from the discharge in liquid to the spark generation is seen as a reduction of resistance. The minimal resistance in the liquid phase is about 13 kΩ, while during the spark generation it decrease from 6 to 3 kΩ as the U_{max} increase from 0.9 to 2.7 kV (curves 4–7). (b) Discharge starts inside the oxygen bubble. Resistance is constant during the discharge and reduces from 5 to 4 kΩ as the U_{max} increase from 0.9 to 2.8 kV.

on the electrode surface results in an increase of the resistance up to the complete disconnection seen on curve 4 (U_{max}=0.9 kV). The gas generation on the surface of the electrode could result from two different processes: the electrolysis of the medium or its evaporation. The threshold energy of the vapor bubble generation should be proportional to the difference between the boiling and the ambient temperatures.[13] We measured the potential at which a switching off of the current was observed [similar to curve 3, Fig. 2(a)] at different temperatures up to the boiling point. No change of this potential with the liquid temperature has been detected. This observation indicates that the gas causing the disconnection of the liquid from the metal is not a water vapor, but probably hydrogen resulting from the electrolysis of water. If the electric field in the gas layer is high enough, the electron avalanche is generated in this layer, that then propagates inside the liquid.[17] The threshold potential of such a discharge generation was about 400 V, the same as the threshold of the glow discharge on the cathode observed when a dc voltage is applied.[18] This second pulse of current started at this voltage at about 350 ns after the first one (curve 4). Resistance during this pulse was about 6 kΩ—substantially lower than that of the first pulse. As the potential increased, the two pulses fused and the resistance reduced to about 3 kΩ (U_{max}=1.1 kV, curve 5). The electron avalanche started earlier as the potential increased and resistance remained constant during the discharge (curves 6,7).

Thus, the discharge process can be divided into the following stages: First—generation of the layer of hydrogen gas on the surface of electrode at the beginning of the discharge. Second—electric breakdown and electron avalanche generation starting in the gas layer and propagating into the liquid medium. At this stage water is overheated and this results in the water vapor bubble growth. When the collapsing vapor bubble moves away together with the generated hydrogen gas a slow charge of the capacitor occurs. At this stage the electrode has a low (a few volts) positive potential, and thus, the oxygen gas is generated on its surface. This gas accumulates into small (about 50 μm) bubble that slowly rise up in the solution. If the pulse repetition rate is so high (10–20 Hz) that the oxygen bubble could not dissolve or move away of the electrode before the next pulse, the following discharge occurs inside the oxygen bubble. The resistance of the discharge starting inside the oxygen bubble located on the electrode [see Fig. 7(b), obtained by division of the corresponding signals (U over I) shown in Fig. 2(c)] was constant during the discharge. This resistance reduced from 5 to 3 kΩ, as the U_{max} increased from 0.9 to 2.8 kV. As the resistivity of the plasma is much lower than that of the electrolyte, the resistance during spark generation phase is determined mainly by the potential drop inside the liquid in the surrounding of the plasma. Thus, it depends mainly on dimensions of the plasma-liquid interface, and not on the wire diameter.

As shown in Fig. 5, dynamics of cavitation bubble is similar to that observed with the ArF excimer laser in a strongly absorbing liquid environment.[1] Generation of the mushroom-like shape at the collapse stage, and ejection of the secondary bubbles in the forward direction results from the influence of the tip on the bubble growth and collapse.[1] Efficiency of the discharge energy conversion to the energy of the cavitation bubble is about 12%, which is about twice as low as that obtained with the Nd:YAG and ArF excimer

laser.[1] On the other hand, the threshold energy of cavitation bubble generation — 3.3 μJ — obtained with an electric discharge is at least five times lower than that obtained with fiber delivery-based laser systems applied to vitreoretinal surgery.[1,2,14] Both these parameters, the threshold and the efficiency of the bubble generation are determined by the primary heat distribution in space, which is different in these two cases. In vitreoretinal surgery cavitation bubbles of about 0.4–0.5 mm in diameter are generally used.[5,11,14,19] Electric discharge generates such bubbles at the energies of 32 and 62 μJ, respectively, which is lower than the corresponding laser pulse energies.[1,2,10,14]

One specific aspect of the electric discharge application for generation of cavitation bubble is a possible electroporation of the adjacent tissue by a strong electric field. The distance r from the electrode at which the electric field becomes lower than the threshold value E_{th} during the discharge with the starting potential U can be estimated as following:

$$r = \sqrt{\frac{U \cdot a}{k \cdot E_{th}}},$$

where a is the radius of the electrode, $k=1$ at $r \ll D(D/2)$ or $k=2$ at $r \gg D(D/2)$ and D is the diameter of the insulator at the exit plane of the tip. Assuming $U=2$ kV, $a=12$ μm, and $E_{\text{th}}=1$ kV/cm,[20] we obtain $r = 0.35$ mm. The data for the threshold electric field of the electropermeabilization[20] was obtained for application of 10 pulses with 100 μs duration. Electropermeabilization is a transient phenomenon, and generally do not influence cell viability at such conditions. To cause unrepairable cell injury higher electric fields are required.[20] In addition, much shorter—submicrosecond—pulses are applied in our case, so the distance of about 0.35 mm is, probably, an overestimation of safe distance of application of the electrodes with respect to possible electropermeabilization effect. However, even this estimation results in lower value than the effects caused by cavitation[2,4] during the laser applications in retinal surgery. The efficiency of cutting of various ocular tissues, as well as the safety issues such as an extent of collateral damage in the vicinity to the application site and the delayed physiological response is a matter of an ongoing investigation in our laboratory.[22]

The similarity of the energies, the bubble dimensions and dynamics indicates that the described electrical device has a potential to become a cost-effective alternative to vitreoretinal surgical equipment based on the fiber-delivered pulsed lasers. In addition, electric discharge may allow the investigation of the mechanics of the tissue disruption by cavitation bubble, as it enables the independent variation of the rise time, peak power, pulse duration and shape along with dimensions of the interaction zone. Such variations are difficult to achieve with lasers, and it could be very helpful for evaluation of the roles of such parameters as pressure, deformation, boundary velocity and acceleration in the process of soft tissue cutting.

ACKNOWLEDGMENTS

The authors thank Galina Fish and Rima Glazer for much help with preparation of the microelectrodes.

APPENDIX

To estimate the parameters of the required electric pulse the shape of the electrode can be assumed for simplicity as half-a-sphere. The resistance of the solution between such electrode of radius $\boldsymbol{a}$ and the large electrode at infinity is[21]

$$R = \frac{\gamma}{2\pi \cdot a}, \tag{A1}$$

where γ is the resistivity of the solution. The current density near the electrode on a surface of half-a-sphere with radius r is

$$j = \frac{U}{2\pi \cdot R \cdot r^2} = \frac{Ua}{\gamma \cdot r^2},$$

where U is the electrode potential. Thus the density of the Joule heat power in this area will be

$$w_{\text{joul}} = j^2 \cdot \gamma = \frac{U^2 \cdot a^2}{\gamma \cdot r^4}.$$

This power will heat the water with a rate

$$\frac{dT}{dt} = \frac{U^2 \cdot a^2}{\gamma \cdot \rho \cdot C r^4},$$

where ρ is the water density (1 g/cm^3), and C is its heat capacity [4.19 J/(g$\cdot$ grad)]. At the electrode surface ($r=a$) this rate is

$$\frac{dT}{dt} = \frac{U^2}{\gamma \cdot \rho \cdot C a^2}. \tag{A2}$$

The total energy of the pulse that will dissipate as heat in the solution will be

$$E = \int_0^\infty \frac{U^2}{R}\, dt,$$

After substituting Eqs. (A1) and (A2) under the integral we obtain

$$E = 2\pi a^3 C \rho \Delta T, \tag{A3}$$

where ΔT is the total temperature rise in the surface layer of the liquid during the pulse. The threshold energy of cavitation bubble formation is the energy required for heating of water to 100 °C.[13] Thus, the threshold energy of about 5 μJ corresponds to the electrode radius a of about 13 μm (assuming room temperature as 20 °C). As the resistivity $\gamma \approx$ 70 Ω cm (for Hartmann's solution), the resistance of the solution R with such an electrode will be about 4.3 kΩ. As the electrode is not a hemisphere, but rather an inlaid disk, the actual resistance will be higher by factor $\pi/2$.[21] Thus, it will be about 6.8 kΩ. On the other hand, as the resistivity of the solution reduces with temperature, in different areas of the heated zone it will be different, so for accurate calculations this effect should also be taken in consideration.

The upper estimation of the influence of the heat transfer from water to the electrode during the electric pulse on the threshold energy of cavitation bubble generation can be obtained by modeling the experimental situation by a one dimensional heat transfer inside the metal rod with a constant temperature at its end equivalent to 100 °C during the pulse. This energy can be estimated as follows:

$$Q = 2a^2 \Delta T \sqrt{\pi C_h \rho \lambda \tau}, \tag{A4}$$

where the heat capacity $C_h = 0.134$ J/g grad, density $\rho = 21.5$ g/cm^3, and the heat conductivity $\lambda = 70$ W/m grad for platinum. In order to limit this heat transfer at the level of 5% of the threshold energy, the pulse duration (τ) should not exceed 0.3 μs. The heat transfer inside water during the same time will be even lower. Thus, the influence of the heat transfer on the threshold energy of vaporization will be negligible in these conditions.

Duration of the discharge of capacitance C on the resistor R is $\tau = RC$, so for obtaining $\tau < 0.3$ μs, C should not exceed 40 pF. For obtaining an energy $E = 5$ μJ, the charging potential U_0 of the capacitance C will be

$$U_0 = \sqrt{2E/C} \approx 500 \text{ V}. \tag{A5}$$

[1] I. Turovets, D. Palanker, Y. Kokotov, I. Hemo, and A. Lewis, J. Appl. Phys. **79**, 2689 (1996).
[2] P. D. Brazitikos, D. J. D'Amico, M. T. Bernal, and A. W. Walsh, Ophthalmology **102**, 278 (1994).
[3] A. Vogel, S. Busch, K. Jungnickel, and R. Birngruber, Lasers Surg. Med. **15**, 32 (1994).
[4] D. Palanker, I. Turovets, and A. Lewis, Proc. SPIE **2681**, 220 (1996).
[5] C. P. Lin, D. Stern, and C. A. Puliafito, Invest. Ophthalmol. Visual Sci. **31**, 2546 (1990).
[6] P. E. Dyer, M. E. Khosroshahi, and S. J. Tuft, Appl. Phys. B **56**, 84 (1993).
[7] T. Juhasz, X. H. Hu, L. Turi, and Z. Bor, Lasers Surg. Med. **15**, 91 (1994).
[8] R. Vorreuther, R. Corleis, T. Klotz, P. Bernards, and U. Engelmann, *J. Urology* **153**, 849 (1995).
[9] R. Lemery, T. K. Leung, E. Lavallee, A. Girard, M. Talajic, D. Roy, and M. Montpetit, Circulation **83**, 279 (1991).
[10] D. Palanker, I. Hemo, I. Turovets, H. Zauberman, and A. Lewis, Invest. Ophthalmol. Visual Sci. **35**, 3835 (1994).
[11] C. P. Lin, Y. K. Weaver, R. Birngruber, J. G. Fujimoto, and C. A. Puliafito, Lasers Surg. Med. **15**, 44 (1994).
[12] G. Fish, O. Bouevitch, S. Kokotov, K. Lieberman, D. Palanker, I. Turovets, and A. Lewis, Rev. Sci. Instrum. **66**, 3300 (1995).
[13] E. D. Jansen, T. G. van Leeuwen, M. Motamedi, C. Borst, and A. J. Welch, J. Appl. Phys. **78**, 564 (1995).
[14] D. Palanker, I. Turovets, A. Lewis, Lasers Surg Med. (in press).
[15] F. R. Young, *Cavitation* (McGraw-Hill, England, 1989), pp. 13–16.
[16] H. M. Jones and E. E. Kunhardt, J. Appl. Phys. **78**, 3308 (1995).
[17] H. M. Jones and E. E. Kunhardt, J. Appl. Phys. **77**, 795 (1995).
[18] A. Hickling, ''Electrochemical Processes in Glow Discharge at the Gas-Solution,'' *Interface*, edited by J. O'M Bockris and B. E. Conway in *Modern Aspects of Electrochemistry No. 6* (Plenum, New York, 1971) Ch. 5, pp. 329–373.
[19] I. Hemo, D. Palanker, I. Turovets, A. Lewis, and H. Zauberman, Invest. Ophthalmol. Vis. Sci. (in press).
[20] J. Teissie and M. P. Rols, ''Manipulation of Cell Cytoskeleton Affects the Lifetime of Cell Membrane Electropermeabilization,'' in *Electrical Injury*, edited by R. C. Lee, M. Capelli-Schellpfeffer and K. M. Kelley (Annals of the N.Y. Academy of Sciences, New York, 1994), Vol. 720, pp. 98–110.
[21] B. R. Scharifker, ''Microelectrode Techniques in Electrochemistry,'' in *Modern Aspects of Electrochemistry*, edited by J. Bockris and B. E. Conway (Plenum, New York, 1992), p. 472.
[22] D. Palanker, I. Turovets, and A. Lewis, Proc. SPIE **2971** (in press) (1997).